YMTHE, Volume *29*

Supplemental Information

Leukemic extracellular vesicles induce chimeric antigen receptor T cell dysfunction in chronic lymphocytic leukemia

Michelle J. Cox, Fabrice Lucien, Reona Sakemura, Justin C. Boysen, Yohan Kim, Paulina Horvei, Claudia Manriquez Roman, Michael J. Hansen, Erin E. Tapper, Elizabeth L. Siegler, Cynthia Forsman, Sydney B. Crotts, Kendall J. Schick, Mehrdad Hefazi, Michael W. Ruff, Ismail Can, Mohamad Adada, Evandro Bezerra, Lionel Aurelien Kankeu Fonkoua, Wendy K. Nevala, Esteban Braggio, Wei Ding, Sameer A. Parikh, Neil E. Kay, and Saad S. Kenderian

Table S1. Characteristics of Untreated CLL Patients.					
ID	**FISH**	**RAI Stage**	**IgVH Status**	**Sex**	**EV(x10^6)/uL**
1	13q	0	unmutated	male	30.2
2	13q	IV	mutated	male	52.1
3	13q	0	unmutated	male	48.1
4	13q	II	unmutated	male	20.9
5	13q	0	-	female	44.4
6	-	I	-	female	12.6
7	11q	0	unmutated	male	20.9
8	Normal	0	mutated	male	18.4
9	11q	0	mutated	male	38.8
10	13q	0	mutated	male	23.2
11	Normal	-	mutated	female	14.2
12	Normal	0	mutated	male	10.8
13	13q	0	-	male	9.1
14	Normal	0	-	female	26.8
15	Tri-12	-	mutated	female	43.6
16	-	0	-	male	32.9
17	13q	0	mutated	male	58.0
18	-	I	-	female	56.3
19	-	0	-	female	5.5
20	13q	0	-	male	16.4
21	-	I	unmutated	male	13.4
22	-	I	unmutated	male	26.7
23	13q	0	uninterpretable	male	12.4
24	13q	IV	mutated	female	17.2
25	Normal	IV	mutated	male	27.9
26	13q	0	mutated	male	20.6
27	-	II	-	male	30.3
28	Normal	0	mutated	male	17.4
29	13q	0	mutated	male	36.2
30	-	I	-	male	16.8
31	Normal	0	mutated	male	20.3
32	-	0	mutated	male	62.4
33	Normal	I	unmutated	male	52.9
34	13q	0	unmutated	female	18.6
35	Tri-12	0	unmutated	male	21.7
36	-	0	mutated	female	33.1
37	13q	0	mutated	male	19.3
38	13q	0	mutated	female	66.6
39	13q	II	mutated	female	27.5
40	Normal	0	unmutated	male	25.2
41	13q	0	mutated	female	10.6
42	13q	0	unmutated	male	31.0
43	13q	0	mutated	female	10.8
44	Normal	0	mutated	female	10.0
45	13q	0	mutated	male	29.3
46	13q	0	mutated	female	17.1
47	-	0	mutated	male	50.7
48	-	0	-	male	34.6
49	13q	0	unmutated	male	60.9
50	Normal	0	unmutated	male	130.0

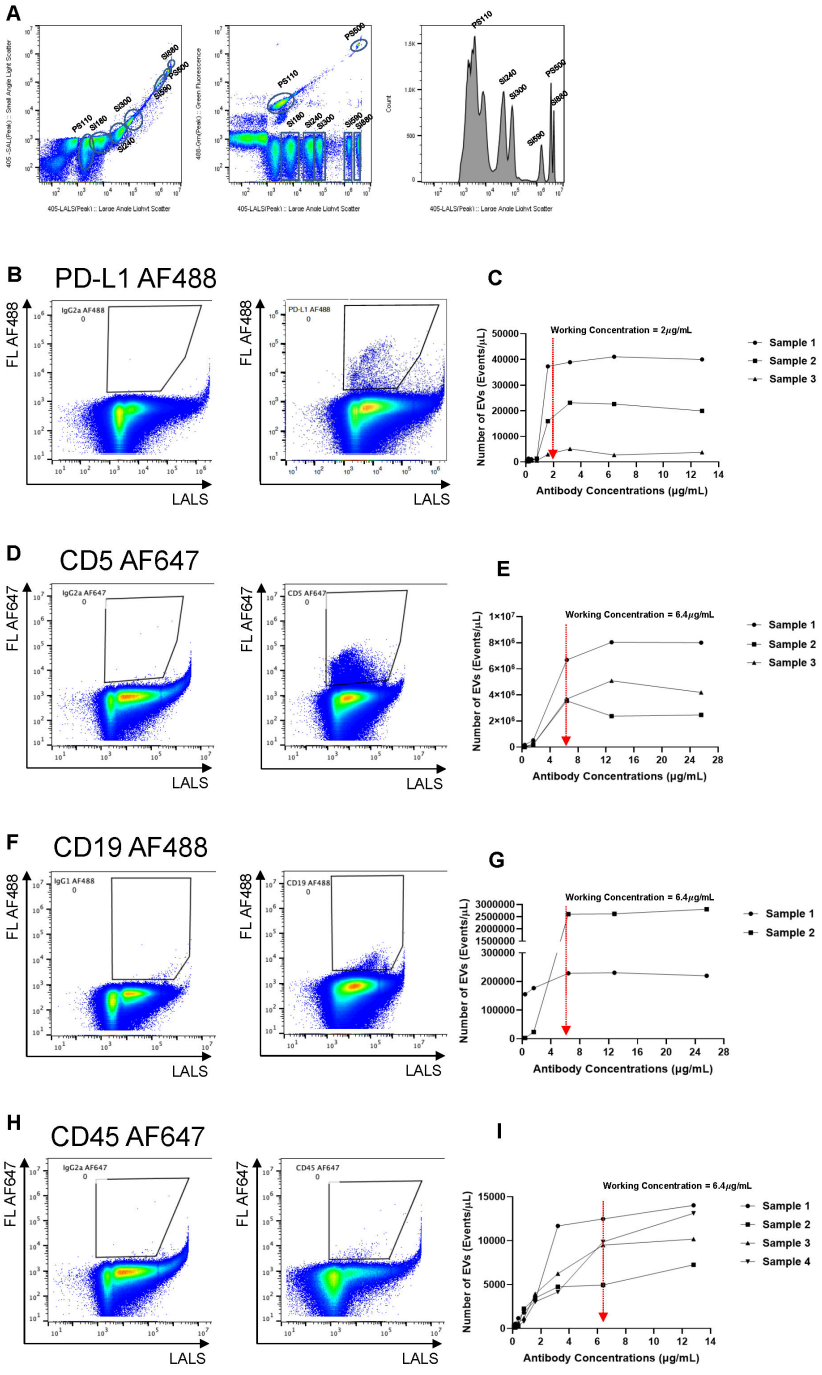

Supplemental Fig. S1 | Nanoscale flow cytometric detection of EV subpopulations from platelet-poor plasma. A) Representative scatterplots of a polystyrene and silica bead mixture detected by nanoscale flow cytometry. Two fluorescent polystyrene bead populations PS110=110nm, PS500=500nm and 5 silica bead populations (180, 240, 300, 590, 880 nm). Left panel represents light-scatter detection with LALS in X-axis and SALS in Y-axis. Middle panel represents LALS in X-axis and fluorescence (FL488) in Y-axis. Right panel represents LALS in X-axis and bead count in Y-axis. **B-I)** Representative scatterplots of a platelet-poor plasma sample incubated with fluorescent antibodies against PD-L1 **(B)**, CD5 **(D)**, CD19 **(F)**, CD45 **(H)** or antibody-matched isotypes. Gates represent events acquired as EVs positive for each marker. Antibody titration curves **(C, E, G, I)** were obtained from nanoscale flow cytometric detection of EVs from normal individual-derived platelet-poor plasma (n=2-4) incubated with increasing concentrations of antibodies or antibody-matched isotypes. Red arrows indicate antibody concentrations used for EV immunophenotyping of patient plasma.

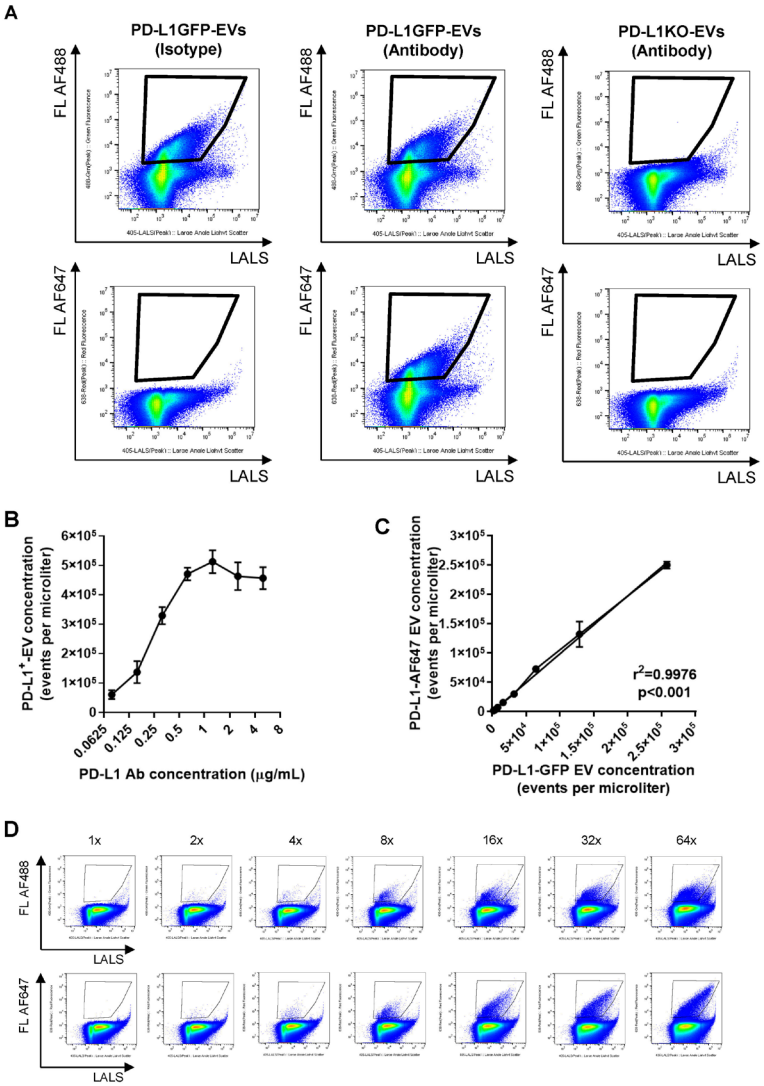

Supplemental Fig. S2 | Evaluation of the performance of nanoscale flow cytometric detection of PD-L1-positive EVs from patient plasma. A) Scatterplots of nanoscale flow cytometric detection of PD-L1-positive EVs isolated from 786-O cells overexpressing PD-L1GFP. PD-L1GFP-positive EVs were incubated with antibody-matched isotype (left panel) or anti-PD-L1 (middle panel). EVs isolated from PD-L1 knockout cells were used as negative control (right panel). **B)** Antibody titration curve for PD-L1 antibody using PD-L1^{+}-EVs isolated from 786O cells. A fixed concentration of approximately 500,000 PD-L1^{+}-EVs determined by nanoscale flow cytometry was used as reference. **C)** Linear regression model showing correlation between concentrations of PD-L1GFP-EVs and antibody-labeled PD-L1EVs from dilutions of PD-L1GFP-EVs spiked-in 3 platelet-poor plasma (normal individuals). Coefficient of determination (r^2) and one-tailed p-value test was performed. **D)** Representative scatterplots of nanoscale flow cytometric detection of PD-L1-positive EVs spiked-in a platelet-poor plasma. Scatterplots for GFP detection (upper row) and antibody detection (lower row) are shown.

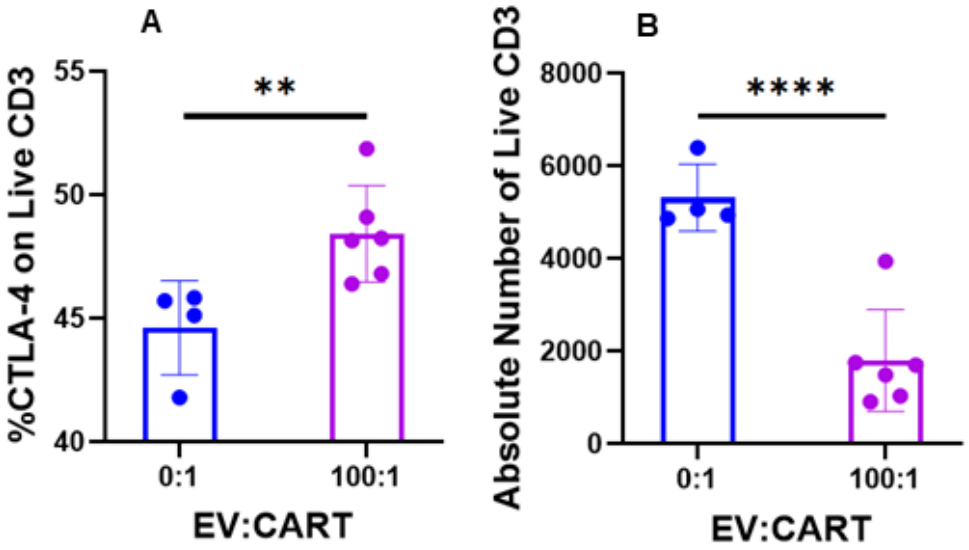

Supplemental Fig. S3 | CLL-Derived EVs impact TCR-specific proliferation and inhibitory receptor modulation of CART19 cells. A) Inhibitory receptor expression on CART cells activated by CD3:CD28 beads is upregulated by CLL-derived EVs. CART19 were co-cultured for 24 hours with a 3:1 bead:cell ratio and 100:1 EV:CART (** p <0.01, one-way ANOVA; error bars, SEM; 3 biological and 2 technical replicates, 2 experiments). **B)** TCR-specific proliferation of CART19 is significantly decreased after 6 hours of co-culture with CLL-derived EVs. CART19 were co-cultured for 24 hours with a 3:1 bead:cell ratio and 100:1 EV:CART (**** p <0.0001, one-way ANOVA; error bars, SEM; 3 biological and 2 technical replicates, 2 experiments).

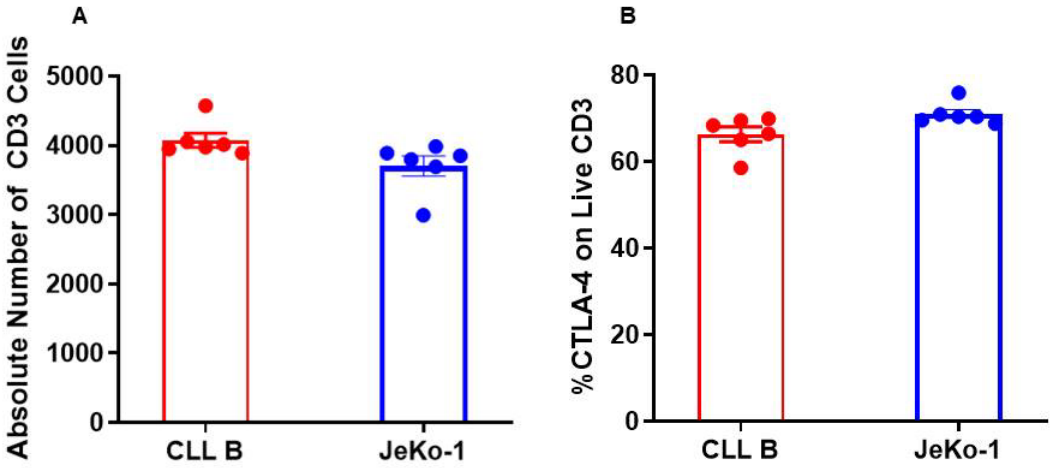

Supplemental Fig. S4 | CLL B cells and JeKo-1 showed similar alteration of CART19 antigen-specific proliferation and inhibitory receptor expression. Example of antigen-specific proliferation **(A)** and CTLA-4 expression **(B)** on CART19 co-cultured with CLL-derived EVs for 24 hours with CLL B cells or JeKo-1. Experiments were performed with 3 biological replicates of CLL-derived EVs at 4 different doses and 2 technical replicates. Results between CLL B cells and JeKo-1 were comparable and thus JeKo-1 was used as a controlled proxy in the CLL model.

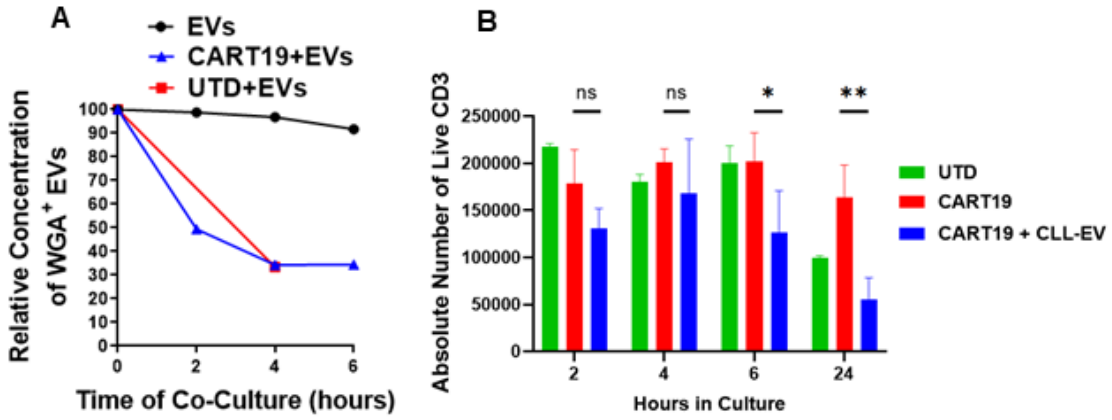

Supplemental Fig. S5 | CLL-Derived EVs significantly impact antigen-specific proliferation of CART19 cells after 6 hours of co-culture. A) EV concentration declines in the presence of CART19 or untransduced T (UTD) cells within 2-to-6 hours of co-culture. EVs, CART19 or UTD, and CLL B cells co-cultured at a 100:1:1 ratio. Percentage of EVs in suspension measured by nanoscale flow cytometry at 0, 2, 4, and 6 hours. **B)** Antigen-specific proliferation of CART19 is significantly decreased after 6 hours of co-culture with CLL-derived EVs. EVs were co-cultured with CART19 cells at a 100:1 ratio for 0, 2, 6, and 24 hours and then activated with the $CD19^+$ cell line JeKo-1.

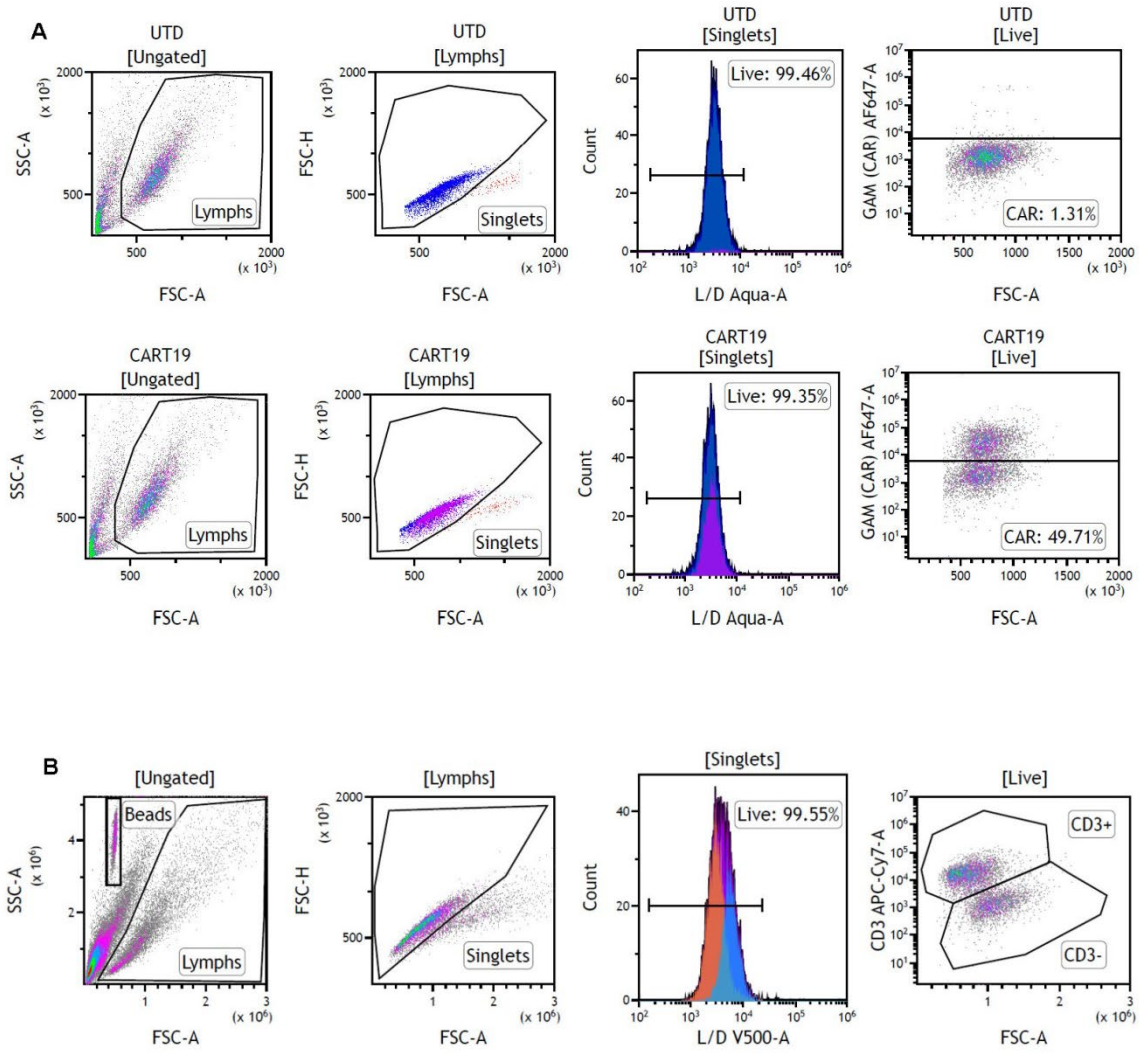

Volume Acquired (uL)	90.00
Bead Events	2366
CD3+ Events	3402
Abs CD3+ (vol)	7560.27
Abs CD3+ (beads)	7764.50
CD3- Events	2295
Abs CD3- (vol)	5100.18
Abs CD3- (beads)	5237.95

$$\frac{\#events\ (population)}{volume\ acquired\ (uL)}\ x\ total\ volume\ (uL) = \ absolute\ number\ of\ cells\ (vol)$$

$$\frac{\#events\ (population)}{\#bead\ events}\ x\ \frac{\#beads\ added}{total\ volume\ (uL)}\ x\ total\ volume\ (uL) = \ absolute\ number\ of\ cells\ (beads)$$

Supplemental Fig. S6 | Gating strategy for flow cytometry. A) Gating strategy to measure CAR expression on T cells. Goat anti-mouse F(ab')2 antibody (GAM) was used with live/dead aqua to detect CAR expression on CART19 cells. Cells were gated on FSC/SSC followed by singlet discrimination and live cells. Negative gates for CAR expression were set based on untransduced (UTD) T cells. **B)** Gating strategy to quantify CART19 cells and target cells. Cells were gated on FSC/SSC followed by singlet and live cell discrimination. CD3 and FSC were used to separate CART19 cells from target cells. Absolute quantification was performed using volumetric measurement. Calculations for both volumetric and bead quantification using CountBright beads are shown.